Scripta Materialia 133 (2017) 75–78

Contents lists available at ScienceDirect

Scripta Materialia

journal homepage: www.elsevier.com/locate/scriptamat

Regular article

# On the occurrence of a eutectic-type structure in solidification of Al-Zr alloys

F. Wang [a], D.G. Eskin [a,*], A.V. Khvan [b], K.F. Starodub [b], J.J.H. Lim [c], M.G. Burke [c], T. Connolley [d], J. Mi [e]

[a] Brunel University London, Brunel Centre for Advanced Solidification Technology, Kingston Lane, Uxbridge UB8 3PH, United Kingdom
[b] National University of Science and Technology MISIS, Thermochemistry of Materials SRC, Leninsky Prosp. 4, Moscow, 119049, Russian Federation
[c] University of Manchester, Materials Performance Centre, Manchester M13 9PL, United Kingdom
[d] Diamond Light Source Ltd., Harwell Science & Innovation Campus, Didcot OX11 0DE, United Kingdom
[e] University of Hull, School of Engineering, Hull HU6 7RX, United Kingdom

ARTICLE INFO

*Article history:*
Received 31 January 2017
Received in revised form 17 February 2017
Accepted 18 February 2017
Available online xxxx

*Keywords:*
Eutectic solidification
Solidification microstructure
Differential thermal analysis (DTA)
Electron diffraction
Al-Zr

ABSTRACT

For the first time, experimental evidence is presented for the occurrence of a eutectic reaction in dilute Al-Zr alloys solidified at cooling rates from 0.5 to 5 K/s. Particles which formed at grain boundaries during solidification were confirmed by electron diffraction analysis to be the equilibrium tetragonal $DO_{23}$ $Al_3Zr$ phase. Differential thermal analysis showed a thermal arrest at 658–659 °C, i.e. below the melting point of pure Al, which indicated the presence of a eutectic reaction.


Zirconium is added to aluminium alloys for several purposes: to prevent or control recrystallization [1], to enhance mechanical properties and thermal stability while retaining electrical conductivity [2], and to control grain size during solidification [3]. In the first two cases, supersaturation of the Al solid solution is achieved during solidification and the metastable $L1_2$ $Al_3Zr$ phase precipitates during annealing, pinning dislocations and subgrain boundaries [1]. In the last case, primary crystals of the equilibrium $Al_3Zr$ phase act as nucleating substrates for Al grains [4]. Non-equilibrium solidification of Al-rich Al-Zr alloys typically results in either formation of a supersaturated solid solution of Zr in Al or the formation of the metastable $Al_3Zr$ phase [5]. When designing alloys for these applications, rather small concentrations of Zr are used, typically below 0.2 wt%; and the peritectic reaction in the Al corner of the Al–Zr binary phase diagram is assumed: $L + Al_3Zr \rightarrow (Al)$ at 661 °C [6] with the peritectic point at 0.28 wt% Zr and the maximum liquid solubility of Zr in (Al) 0.11 wt% at 661 °C [7]. However, most of the work on the equilibria in the Al corner of the Al-Zr phase diagram has been done by assessment rather than by direct measurements [6].

In this study we present for the first time experimental evidence of a probable eutectic reaction occurring in the Al corner of the Al-Zr system, instead of the conventionally accepted peritectic reaction.

Evidence for a eutectic-type reaction arose during work to study the solidification microstructures of Al–Zr alloys, containing 0.1, 0.15, 0.3, 0.4, and 0.5 wt% Zr. These alloys were made by the UK group in a graphite crucible and electric resistance furnace using 99.99% pure Al and an Al–10 wt% Zr master alloy. The master alloy was added to the molten aluminium at 900 °C and the melt was isothermally held for 1 h with intermittent stirring before solidifying either in a graphite crucible in air (1 K/s) or by pouring into a copper wedge mould preheated to 500 °C, enabling a range of cooling rates from 3 to 12 K/s, as recorded by K-type thermocouples. Metallographic samples were cut from the bottom parts of the castings, ground and polished using standard techniques and examined in scanning (SEM, Zeiss SUPRA35V) and transmission (TEM, JEOL 2100) electron microscopes. Four foil samples approximately 80 to 90 nm-thick were also prepared by focused ion beam (FIB, FEI Helios 660) from the areas of interest and used for phase identification by TEM. In addition, deep etching of some samples with NaOH water solution was performed to remove the Al matrix, thereby revealing the 3D morphology of the intermetallic particles.

In addition, alloys containing 0.4 and 1 wt% Zr were prepared independently by the Russian group using 99.99% pure Al and 99.99% pure Zr at 1000 °C, allowing for melt homogenisation for 2 h before solidification in a graphite crucible in air. Samples from the casting were cut and used for metallographic and differential thermal analysis (DTA/DSC Labsys Setaram). Prior to the measurements, the apparatus was calibrated using high-purity metal standards (99.999% Pb, 99.99% Al,

* Corresponding author.
*E-mail address:* dmitry.eskin@brunel.ac.uk (D.G. Eskin).

http://dx.doi.org/10.1016/j.scriptamat.2017.02.027

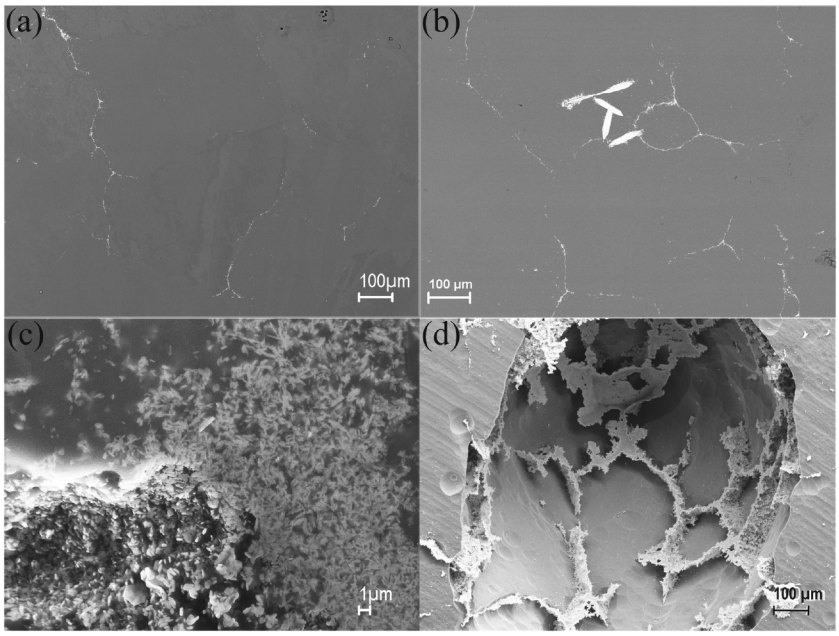


**Fig. 1.** Secondary electron images of grain-boundary particles formed during solidification in Al–0.4 wt% Zr alloys at a cooling rate of 5 K/s (a) and 1 K/s (b–d): a, b, general view; c, higher magnification of grain boundary particles; and d, deep etching of the matrix.

99.99% Cu, 99.99% Ag). Using reproducibility of the calibration data, the instrumental error of temperature measurements was estimated as ±0.04 K. The samples for these measurements were kept in closed $Al_2O_3$ crucibles under a continuous 99.995% Ar flow, which was additionally filtered for oxygen. Before the experiments, the DTA/DSC apparatus was pumped out to $10^{-5}$ atm and flushed with Ar three times. The heating/cooling rates for calibration and experiments were 5, 1 and 0.5 K/min. Experiments with an empty crucible or pure 99.99% Al as a reference sample were conducted. The heating curves were used to determine the solidus temperatures of the samples at different heating rates as recommended by the DTA guidelines [8].

Metallographic examination of the studied samples reliably revealed the presence of fine intermetallics at dendritic grain boundaries in all samples containing more than 0.15% Zr and solidified at cooling rates below 5 K/s. No intermetallic phases were found at lower Zr concentrations and at higher cooling rates (apparently due to the well-known phenomenon of supersaturation of the Al solid solution with Zr [1]). It is interesting to note that, on decreasing the cooling rate from 5 to 1 K/s, first the intermetallics at grain boundaries appeared and then the primary crystals were formed in addition to the grain-boundary particles as illustrated in Fig. 1a & b. These primary crystals are formed at hyper-eutectic compositions and have been observed in all the studied alloys containing more than 0.15% Zr, which places the eutectic composition somewhere around 0.12–0.15% Zr (similar to the composition above which the primary intermetallics have been usually observed in this system). The fact that the primary particles do not always appear at higher cooling rates is also a well-known experimental fact for these alloys. The eutectic structure is, however, less affected by the cooling rate and has been always observed in the range of cooling rates 1 to 5 K/s.

At a higher magnification, one can resolve very fine (micron and submicron size) particles with a button shape (Figs. 1c and 2a), while deep etching revealed that these particles form a continuous network at grain boundaries (Fig. 1d). The alloys prepared for DTA analysis showed similar microstructures.

The identification of the submicron particles at grain-boundary was performed using energy dispersive X-ray spectroscopy (EDS) spectrum imaging (Fig. 2) in combination with selected-area electron diffraction (SAED) analysis (Fig. 3) in the TEM at 200 kV. EDS maps extracted from the spectrum image datasets (Fig. 2) clearly show that the particles contain the elements Al and Zr. The selected-area diffraction patterns (Fig. 3) obtained at different beam directions for each particle were consistently indexed as tetragonal $DO_{23}$ $Al_3Zr$ particles and the measured d-spacing, interplanar angles and angles between beam directions agree well with published values of tetragonal $DO_{23}$ $Al_3Zr$ [7,9]. Both the EDS data and electron diffraction analyses confirmed that these

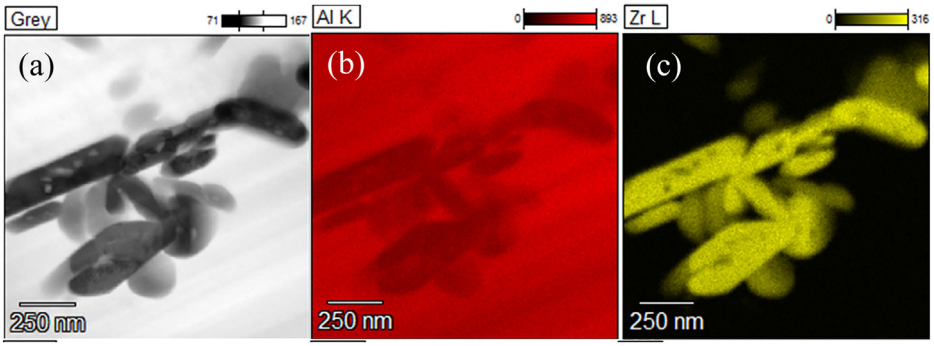


**Fig. 2.** (a) STEM image of intermetallic particles along the grain boundary; and EDS maps showing the elemental distribution of (b) Al and (c) Zr in the particles.

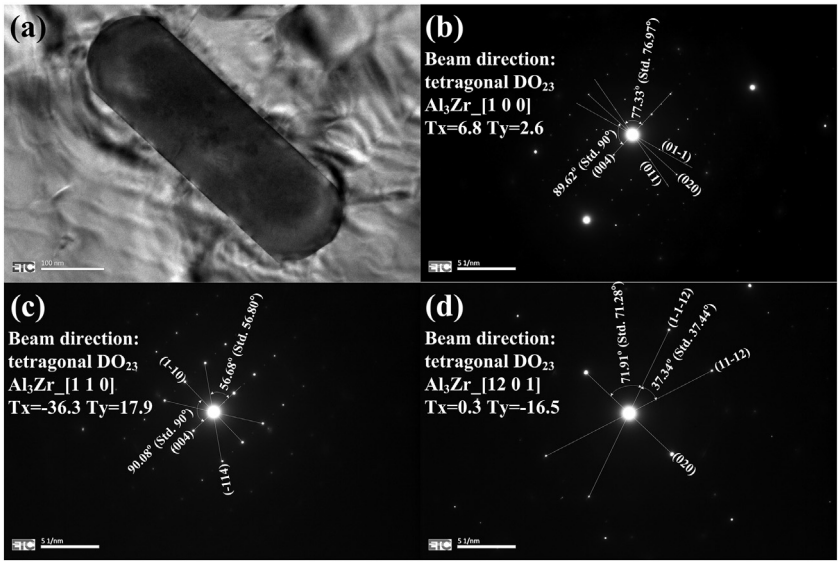


**Fig. 3.** (a) TEM-BF image of a typical intermetallic particle at a grain boundary; (b), (c), and (d) SAED patterns obtained from the intermetallic particle and indexed as tetragonal $DO_{23}$ $Al_3Zr$ with beam directions (BDs): (b) [1 0 0]; (c) [1 1 0] and (d) [12 0 1].

particles are the equilibrium tetragonal ($DO_{23}$) $Al_3Zr$ particles. The faceted shape of these particles is typical of an irregular eutectic [10]. It is necessary to mention that 40 particles were analysed in total, with reproducible and consistent results.

The clear metallographic evidence of the formation of intermetallic particles of the equilibrium phase at grain boundaries during solidification, in a system that is accepted as a peritectic, needs adequate explanation. Various non-equilibrium effects during solidification in a peritectic system may result in the appearance of intermetallic particles at grain boundaries. During solidification, primary intermetallic particles may form in a range of sizes with the larger ones acting as substrates for the aluminium solid solution, while the smaller ones are pushed to the grain boundaries [11]. Another scenario is the so-called banding cycle of peritectic transformation [12], which may result in the formation of intermetallics at the periphery of the aluminium solid solution. These possibilities can be, however, dismissed due to the following results of our DTA analysis that clearly suggest a eutectic type of solidification reaction between Al and $Al_3Zr$.

Table 1 gives a summary of DTA measurements for the Al–1 wt% Zr with an empty ceramic crucible as a reference sample. The Al–Zr and Al columns show melting points for the corresponding materials at the given heating rates. These results show that the Al–1 wt% Zr alloy has a lower melting temperature than pure Al (660.3 °C as measured during calibration), which suggests that the reaction in the Al-rich region is of the eutectic type.

Similar results were obtained in the DTA experiment with Al-Zr alloys, where pure Al was taken as a reference sample.

Fig. 4 shows that the Al–1 wt% Zr melting process results in a negative peak with the onset at 658.5 °C, which is followed by a positive peak caused by the melting of the pure Al sample. The opposite direction of peaks in this curve is a result of superposition of two melting events in different sample holders situated at the opposite sides of the detector (similar to the technique used by Janghorban et al. [14]). The Al–Zr solidus temperature obtained in this experiment corresponds to the values in Table 1. The DTA results for the Al–0.4 wt% Zr alloy showed the same thermal arrests as the Al–1 wt% Zr alloy.

It is worth noting at this point that there have been earlier reports contradicting the peritectic nature of the solidification in the Al-rich alloys. Different authors from different laboratories have, at different times, reported a lower temperature for this reaction, i.e. 655 °C in the USA, 1954 [13] and 656 ± 2 °C in France, 2013 [14], which implies a eutectic reaction, i.e. L → (Al) + $Al_3Zr$. These reports have been dismissed by others as not complying with the thermodynamic modelling of the system. It is important to mention that no metallographic evidence of a eutectic reaction in this system has been reported until now.

The presented results raise a serious concern regarding the validity of the accepted version of the Al–Zr phase diagram. The observed effects may still be of a non-equilibrium nature. For example the difference in the low temperature thermal arrests reported in [13,14] and in our work may reflect the effect of cooling conditions on the reaction temperature. In any way, the observed temperature effects and structures point to the replacement of the peritectic reaction with the eutectic one.

At the moment the nature and stability of the eutectic reaction and phase equilibria are still under detailed experimental investigation. As experimentalists, the UK and Russian groups worked independently

**Table 1**
DTA results for the Al–1 wt% Zr alloy.

| Heating rate, K/min | Melting point, °C |
|---|---|
| 5 | 658.5 |
| 1 | 658.5 |
| 0.5 | 659.1 |

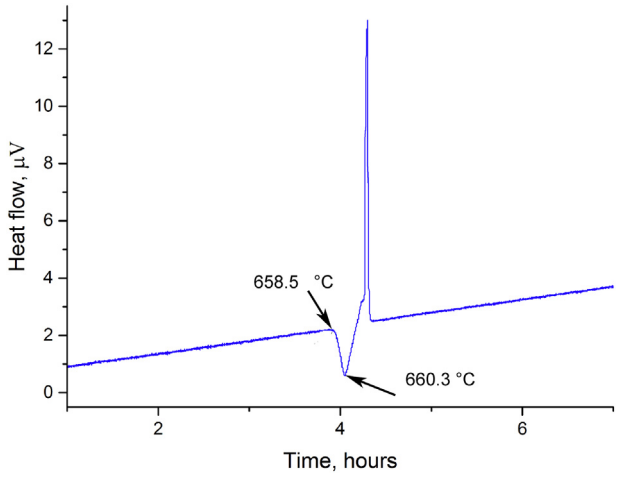


**Fig. 4.** Heating curve for the DTA experiment with the Al–1 wt% Zr alloy, with Al as a reference sample.

and came together as co-authors as we realised that our separate experimental observations were complementary. We are publishing now to encourage others to reproduce our results.

## Acknowledgements

The UK-based authors acknowledge financial support from the Engineering and Physical Sciences Research Council (EPSRC) for the UltraCast project (Grant EP/L019884/1, EP/L019825/1, EP/L019965/1).

## References

[1] N. Ryum, Acta Metall. 17 (1969) 269–278.
[2] N.A. Belov, A.N. Alabin, I.A. Matveeva, D.G. Eskin, Trans. Nonferrous Metals Soc. China 25 (2015) 2817–2826.
[3] T.V. Atamanenko, D.G. Eskin, M. Sluiter, L. Katgerman, J. Alloys Compd. 509 (2011) 57–60.
[4] F. Wang, D. Qiu, Z.-L. Liu, J.A. Taylor, M.A. Easton, M.-X. Zhang, Acta Mater. 61 (2013) 5636–5645.
[5] E. Nes, H. Billdal, Acta Metall. 25 (1977) 1031–1037.
[6] E. Fischer, C. Colinet, J. Phase Equilbr, Differentiation 36 (2015) 404–413.
[7] L.F. Mondolfo, Aluminum Alloys: Structure and Properties, Butterworths, 1976.
[8] W.J. Boettinger, U.R. Kattner, K.-W. Moon, J.H. Perepezko, DTA and Heat-Flux DSC Measurements of Alloy Melting and Freezing, NIST Recommended Practice Guide, NIST, Washington, 2006 Special publication 960-15.
[9] L. Li, Y. Zhang, C. Esling, H. Jiang, Z. Zhao, Y. Zuo, J. Cui, J. Cryst. Growth 316 (2011) 172–176.
[10] J.A. Dantzig, M. Rappaz, Solidification, EPFL Press, Lausanne, 2009 349–366.
[11] L. Greer, P.S. Cooper, M.W. Meredith, W. Schneider, P. Schumacher, J.A. Spittle, A. Tronche, Adv. Eng. Mater. 5 (2003) 81–91.
[12] H.W. Kerr, W. Kurz, Int. Mater. Rev. 41 (1996) 129–164.
[13] D.J. McPherson, M. Hansen, Trans. ASM 46 (1954) 354–371.
[14] A. Janghorban, A. Antoni-Zdziobek, M. Lomello-Tafin, C. Antoin, Th. Mazingue, A. Pisch, J. Therm. Anal. Calorim. 114 (2013) 1015–1020.